Build-Up of Laser Oscillations from Quantum Noise

M. Sargent III, M. O. Scully, and W. E. Lamb, Jr.

Build-up of laser oscillation is expressed in terms of the probabilities $p_n(t)$ that there are n photons in the laser cavity. These probabilities obey a coupled set of difference-differential equations of motion. The method and results of numerical integration of these equations are given here for the initial condition that no photons exist (radiation field vacuum). Corresponding equations of motion for the moments of the photon distribution are derived, and their time dependences are given.

A movie showing the time development of the p_n from an initial vacuum is given on the corners of this issue and can be seen by flipping through the pages.

M. Sargent III is with the Optical Sciences Center, The University of Arizona, Tucson, Arizona 85721.

M. O. Scully is with the Optical Sciences Center and the Department of Physics, The University of Arizona, Tucson, Arizona 85721, and with the Department of Physics and Materials Science Center, Massachusetts Institute of Technology, Cambridge, Massachusetts.

W. E. Lamb, Jr., is with the Department of Physics, Yale University, New Haven, Connecticut 06520.

NGR-07-004-035

Introduction

For many purposes, a classical, transverse electric field expression

$$E(z,t) = E(t)\cos[\nu t + \phi(t)]\sin(Kz) \tag{1}$$

Fig 1

provides an adequate description of laser oscillation (Fig. 1). The wave number is

$$K = n\pi/L \tag{2}$$

for some integer n, where L is the length of the cavity. Under transient conditions, the amplitude E(t) and phase $\phi(t)$ may vary slowly at a rate on the order of ν/Q, where Q is the quality factor of the cavity. According to a treatment by Lamb[1] in which the atoms interact with the classical field according to the laws of quantum mechanics, the amplitude E(t) obeys an equation of motion

$$\dot{E}(t) = E(t)[\alpha - \beta E(t)^2]. \tag{3}$$

Here α is the linear "net gain" coefficient, that is, the coefficient for the difference between the linear gain of the medium and the loss of the cavity. The coefficient β leads to a reduction in the net gain and results from saturation of the medium. From Eq. (3) one obtains the steady-state intensity I as

$$I = E^2 = \alpha/\beta. \tag{4}$$

In general the semiclassical theory has enjoyed excellent quantitative agreement with experiment.

There are, however, several features of laser operation that cannot be understood with a theory in which the electric field is treated classically. First, the linewidth of the field is zero classically although physically (and quantum mechanically) it has a small, finite value. Second, the field cannot build up from a zero value (E = 0) according to the

equation of motion (Eq. (3)). Physically, the laser does build up from zero (photon vacuum) because of spontaneous emission, a quantum mechanical phenomenon. Third, the usual semiclassical treatment does not provide the statistical distribution of energy stored in the laser cavity, that is, the photon statistics. These statistics are required for a proper discussion of the distribution of photoelectrons ejected in a photodetector by laser light. Fourth, Eq. (4) predicts a sharp threshold whereas observation reveals a gradual change.[2]

In this paper, we discuss the buildup of oscillation from the vacuum and some aspects of the photon statistics using results from a fully quantum mechanical theory of the laser.[3] Although the derivations contained in that work require the use of quantum statistical techniques, the results that we will use in the present paper have a simple physical interpretation, and our discussion can be followed by those having little exposure to quantum mechanics and laser theory.[4]

Photon Number Probabilities

Most of our discussion involves the probability $p_n(t)$ that there are n photons in the laser cavity. For example, if no photons are present,

$$p_0 = 1 \text{ and } p_n = 0 \text{ for } n > 0. \tag{5}$$

The photon distribution for filtered thermal light is given by

$$p_n = \exp[-n\hbar\Omega/(k_B T)]\ \{1 - \exp[-\hbar\Omega/(k_B T)]\}, \tag{6}$$

where Ω is the angular frequency of the radiation, k_B is Boltzmann's constant, and T is the absolute temperature. The statistical distribution for coherent light is a Poisson distribution for which

$$p_n = \langle n \rangle^n\ e^{-\langle n \rangle}/n!, \tag{7}$$

where the average number of photons

$$\langle n \rangle = \sum_{n=0}^{\infty} n\, p_n. \tag{8}$$

Fig 2

The statistics for thermal and coherent light are plotted in Fig. 2.

In a laser, the photon distribution is determined by the steady-state solution to the equations of motion for the photon number probabilities

$$\dot{p}_n(t) = -[A - B(n+1)]\ (n+1)p_n(t) + [A - Bn]n\ p_{n-1}(t) - Cn\ p_n(t) + C(n+1)p_{n+1}(t). \tag{9}$$

Here A is the linear gain coefficient, C is the loss coefficient (the semiclassical coefficient α in Eq. (3) corresponds to the difference ½(A-C)), and B is the saturation coefficient[5] (β in Eq. (3) corresponds to $(1/8)(\hbar\nu)^{-1}\epsilon_0 VB$). Under "Numerical Results" we will discuss a numerical analysis of these equations as they describe the buildup of laser oscillation from the vacuum (Eq. (5)). First, however, we will summarize the results obtained in Ref. 3 when the steady-state condition

$$p_n(t) = 0 \tag{10}$$

was imposed.

For this, the equations of motion (Eq. (9)) reduce to the equivalent first-order difference equations

$$[A - Bn]n\ p_{n-1} - Cnp_n = 0 \tag{11}$$

$$[A - B(n+1)]\ (n+1)p_n - C(n+1)p_{n+1} = 0. \tag{12}$$

This reduction of Eq. (9) can be seen by inspection of Fig. 3 in which for steady state the flow of probability due to stimulated emission ($(A-Bn)np_{n-1}$-like terms) is balanced

by that due to cavity losses (Cnp_n-like terms). The solution of either equation is

$$p_n = Z^{-1} \prod_{k=0}^{n} [(A-Bk)/C], \tag{13}$$

where the normalization constant is given by

$$Z = \sum_{n=0}^{\infty} \prod_{k=0}^{n} [(A-Bk)/C]. \tag{14}$$

Fig 4

The distribution of Eq. (13) is graphed in Fig. 4 for three values of excitation.

Below threshold the nonlinear terms with B can be dropped, and the distribution of Eq. (13) becomes that for a blackbody

$$p_n = [1 - A/C]\ (A/C)^n \tag{15}$$

for which the effective temperature T is defined by (compare Eq. (15) with Eq. (6))

$$\exp[-\hbar\Omega/(k_B T)] = A/C. \tag{16}$$

Above threshold, one finds from Eq. (8) that

$$\langle n\rangle = [(A/B) - 1] \sum_{n=0}^{\infty} p_n - (C/B) \sum_{n=0}^{\infty} [A - B(n+1)] C^{-1} Z^{-1} \prod_{k=0}^{n} [(A - Bk)/C]$$

$$= (A/B) - 1 - (C/B)(1 - p_0)$$

$$\cong (A - C)/B, \tag{17}$$

where the approximation in the last line is valid when $\langle n\rangle \gg 1$. This relation corresponds to the semiclassical intensity of Eq. (4). Using Eq. (17) in Eq. (7), one calculates the graph in Fig. 5 in which laser and Poisson distributions are compared. It can be shown using an exact theory that as the gain is increased indefinitely, the laser distribution approaches that of Poisson.

Fig 5

Moments of the Photon Distribution

The kth moment of the distribution is defined by

$$\langle n^k \rangle = \sum_{n=0}^{\infty} n^k p_n. \tag{18}$$

The first of these (k = 1) is just the average number of photons $\langle n \rangle$ introduced earlier in Eq. (8). The energy in the laser cavity is proportional to this moment. Furthermore, the classical energy is proportional to the electric field intensity. In the classical limit where $\langle n \rangle \gg 1$, one can equate the two values for the energy and obtain the relation

$$\langle n \rangle \hbar\nu = \tfrac{1}{4}\epsilon_0 E^2 V, \tag{19}$$

where V is the volume of the cavity and E^2 is given by Eq. (4). The variance σ is given by

$$\sigma = [\langle n^2 \rangle - \langle n \rangle^2]^{\frac{1}{2}}. \tag{20}$$

The equations of motion for the moments are determined by those for the probabilities p_n. Using Eqs. (9) and (18),

$$\begin{aligned} \frac{d}{dt}\langle n^k(t) \rangle &= \sum_{n=0}^{\infty} n^k \dot{p}_n(t) \\ &= -\sum_{n=0}^{\infty} [A-B(n+1)]\,(n+1)n^k p_n + \sum_{n=1}^{\infty} [A-Bn]\, n^{k+1} p_{n-1} \\ &\quad - C\sum_{n=0}^{\infty} n^{k+1} p_n + C\sum_{n=0}^{\infty} (n+1)n^k p_{n+1}. \end{aligned} \tag{21}$$

The n = 0 terms vanish. Hence, the first and second summations can be combined provided that in the second the subscript n - 1 is renamed n, n is renamed n + 1, and the lower limit is changed to 0. Similarly, one can combine the third and fourth summations by renaming n + 1 to n, and by changing the limit 0 to 1 in the fourth. Then

$$\frac{d}{dt}\left\langle n^k(t)\right\rangle = \sum_{n=0}^{\infty}[A - B(n+1)]\,(n+1)\,[(n+1)^k - n^k]\,p_n$$

$$- C\sum_{n=1}^{\infty} n[n^k - (n-1)^k]\,p_n. \tag{22}$$

Specifically, for the first moment (k = 1),

$$\frac{d}{dt}\langle n\rangle = \sum_{n=0}^{\infty}[A - B(n+1)]\,(n+1)p_n - C\sum_{n=0}^{\infty} np_n$$

$$= (A - C)\langle n\rangle + A - B[\langle n^2\rangle + 2\langle n\rangle + 1]. \tag{23}$$

For the second

$$\frac{d}{dt}\langle n^2\rangle = \sum_{n=0}^{\infty}[A - B(n+1)](n+1)(2n+1)p_n - C\sum_{n=0}^{\infty} n(2n-1)p_n$$

$$= 2(A - C)\langle n^2\rangle + (3A + C)\langle n\rangle + A - B[2\langle n^3\rangle + 5\langle n^2\rangle + 4\langle n\rangle + 1]. \tag{24}$$

Using the binomial theorem in Eq. (22), the general equation is

$$\frac{d}{dt}\left\langle n^k\right\rangle = \sum_{n=0}^{\infty}[A - B(n+1)]\sum_{i=0}^{k-1}\binom{k}{i}(n^{i+1} + n^i)p_n$$

$$- C\sum_{n=0}^{\infty}\sum_{i=0}^{k-1}\binom{k}{i}(-1)^{k-1-i}\,n^{i+1}$$

$$= \sum_{i=0}^{k-1}\binom{k}{i}\{\left\langle n^{i+1}\right\rangle[A - (-1)^{k-1-i}C] + \left\langle n^i\right\rangle A$$

$$- B\left[\left\langle n^{i+2}\right\rangle + 2\left\langle n^{i+1}\right\rangle + \left\langle n^i\right\rangle\right]\}. \tag{25}$$

In the classical limit, the equation of motion for $\langle n\rangle$ in Eq. (22) should have the same form as that for the intensity E^2 because of the energy relation in Eq. (19). From Eq. (3),

$$dE^2/dt = E^2\,[2\alpha - 2\beta E^2]. \tag{26}$$

In this limit, one can neglect 1 compared with $\langle n\rangle$ and $\langle n\rangle$ compared with $\langle n^2\rangle$. Furthermore, the distribution becomes sufficiently peaked so that it acts like a delta function, that is,

$$\langle n\rangle^2 = \sum_{n=0}^{\infty}\sum_{n'=0}^{\infty} nn' p_n p_{n'} = \sum_{n=0}^{\infty}\sum_{n'=0}^{\infty} nn' p_n \delta_{nn'} \cdot$$

$$\equiv \langle n^2\rangle$$

Hence, Eq. (23) for $\langle n\rangle$ reduces to

$$\dot{\langle n\rangle} = (A - C)\langle n\rangle - B\langle n\rangle^2 \tag{27}$$

which has the form of Eq. (25) with $\langle n\rangle$ related to E^2 by Eq. (19). The coefficient relations are the same as those given for Eq. (9). For small $\langle n\rangle$, Eq. (23) reduces to $\dot{\langle n\rangle} \cong A - B$ and predicts buildup from noise, a feature not contained in the semiclassical Eq. (26). We now turn to a numerical analysis of both the equations of motion for the probabilities p_n (Eq. (9)), and those for the moments $\langle n^k\rangle$ (Eq. (24)).

Numerical Results

In this section we discuss the numerical analysis of the difference-differential equations, Eqs. (9) and (25), for the photon number probabilities p_n and moments $\langle k\rangle$, respectively, and give specific results for buildup from vacuum. Both sets of equations are infinite in number and must be truncated to the first N terms for numerical integration. Because the Nth term (p_N or $\langle n^N\rangle$) depends on the (N + 1)th term, an estimate of the latter is required.

For the p_n, a satisfactory estimate is given by

$$p_{N+1} = (p_N/p_{N-1})p_N. \tag{28}$$

More sophisticated formulas sometimes yield a p_{N+1} greater than p_N and subsequent divergence. Here the number of terms, N, is taken sufficiently large so that p_N is less than some prescribed number, say 10^{-6}. The initial vacuum is described by the conditions

$$p_0 = 1, p_n = 0 \text{ for } n > 0. \tag{29}$$

Hence, the cutoff index N can be taken very small initially and then gradually increased as the corresponding moments assume values larger than the cutoff minimum. In the course of numerical integration, some p_n beyond the peak but before the cutoff p_N acquire either negative values or values greater than a predecessor. Because these values are nonphysical and lead rapidly to instability, they must be recalculated starting with the first erroneous entry and concluding with the cutoff p_N, inclusively. For this purpose the extrapolation formula, Eq. (28), has proved to be satisfactory.

Because of the sensitive relationship between the equations and the extrapolation procedure, a simple first-order integration method containing only one extrapolation value per p_n has been used. Specifically, we have taken

$$p_n(t+h) = p_n(t) + h\,\dot{p}_n(t), \tag{30}$$

where the time interval $h = 0.0015$ μsec for a cavity bandwidth of 1 MHz.

Fig 6

Fig 7

Movie

In Fig. 6 curves of p_n vs n are graphed for representative times, and for an average steady-state photon number $\langle n \rangle = 50$. A more complete presentation of these results has been given at several conferences in the form of a computer movie.[6] In Fig. 7 similar curves are shown for the larger value $\langle n \rangle = 267$. The corresponding computer movie is given in the upper right-hand corners of this issue and can be seen by thumbing through the journal. For both values of $\langle n \rangle$ the peak of the distribution starts with p_0 and progresses outward; it does not originate at some higher value of n. For $\langle n \rangle = 50$, the peak starts out from p_0 at ~8 μsec, while for $\langle n \rangle = 267$, it starts later at ~17 μsec. The steady-state distributions are attained within 1% in 30 μsec for $\langle n \rangle = 50$ and in 45 μsec for $\langle n \rangle = 267$.

Fig 8

A suitable truncation procedure for the moment equations, Eq. (25), is based on the numerical triangle shown for N = 2 in Fig. 8. There an estimate for $\langle n^3 \rangle$ is required and given by setting the last difference to zero, that is,

$$\langle n^3 \rangle = \left[2 \langle n^2 \rangle^{\frac{1}{2}} - \langle n \rangle \right]^3 . \tag{31}$$

In general,

$$\langle n^{N+1} \rangle = \left\{ \sum_{i=1}^{N} (-)^{N-i} \binom{N}{i-1} \langle n^i \rangle^{1/i} \right\}^{N+1} . \tag{32}$$

Fig 9
Fig 10

In Fig. 9 time integrations of $\langle n \rangle$ are given for several truncation levels (N = 2, 3, and 4) along with that resulting from the p_n integration. In Fig. 10 time integrations of the mean square deviation $[\langle n^2 \rangle - \langle n \rangle^2]^{\frac{1}{2}}$ are given using the same scheme. Note that the deviation initially tends to follow that (an exponential) for thermal light and overshoots the final value. It then approaches a value more characteristic of coherent light as saturation plays an increasingly important role.

Acknowledgments

This research is supported in part by the National Aeronautics and Space Administration, in part by the U.S. Air Force Office of Scientific Research, and in part by the National Science Foundation.

References

1. W. E. Lamb, Jr., Phys. Rev. 134, A1429 (1964).

2. F. T. Arecchi, V. Degiorgio, and B. Querzola, Phys. Rev. Letters 19, 1168 (1967). The experimental results of Arecchi et al. agree qualitatively with the theoretical results reported by the present authors both here and at the Fourth International Conference on Quantum Electronics, Phoenix, Arizona, 1966.

3. M. O. Scully and W. E. Lamb, Jr., Phys. Rev. 159, 208 (1967).

4. Results corresponding to those of the present paper but for a smaller steady-state average photon number ($\langle n\rangle=50$) were presented at the Fourth International Conference on Quantum Electronics, Phoenix, Arizona, 1966. Related work for still larger $\langle n\rangle$ will be published by Y. K. Wang and W. E. Lamb, Jr.

5. These equations of motion are given by those for the diagonal elements of the radiation density matrix ρ defined by Eq. (101) in Ref. 3. The form corresponds to the near threshold theory used for Eq. (3) of the present paper.

6. M. O. Scully, W. E. Lamb, Jr., and M. Sargent III, Fourth International Conference on Quantum Electronics, Phoenix, Arizona, 1966; Bull. Am. Phys. Soc. 12, 89 (1967); M. O. Scully, J. Opt. Soc. Am. 60, 721 (1970).

Figure Captions

Fig. 1. Diagram of laser depicting oscillation of transverse electric field E(z,t) given by Eq. (1).

Fig. 2. Graphs of photon number probabilities p_n for blackbody (solid line) and coherent (dashed line) radiation.

Fig. 3. Flow of probability due to stimulated emission (↑) and damping (↓) for finding n photons in laser cavity.

Fig. 4. Graph of steady-state solution of Eq. (13) for three excitation levels: below (solid line), at (dot-dashed line), and above threshold (dashed line).

Fig. 5. Graphs of photon number probabilites p_n vs photon number for a laser 20% above threshold (solid line) and for a Poisson distribution (dashed line) with the same average number of photons (see Eq. (7)).

Fig. 6. Graph of photon number probabilities p_n obtained at times (in order of increasing $\langle n \rangle$) 2, 5, 8, 11, 14, 17, 21 and 24 μsec, starting with an initial vacuum. Laser parameters used in integration of Eq. (9) are A = 1.2, B = 0.004, C = 1.0, yielding by Eq. (17) an average steady-state photon number $\langle n \rangle = (A-C)/B = 50$.

Fig. 7. Graph of photon number probabilites p_n vs photon number n at times (in order of increasing $\langle n \rangle$) 5, 10, 15, 20, 25, 30, 35, 40, 45, 50 and 55 μ sec. Parameters are the same as for Fig. 6 except that the saturation parameter B = A/1600 = 0.00075, yielding $\langle n \rangle = 267$. The choice A/B = 1600 causes the p_n to equal zero when $n > 1600$ (see Eq. (13)). The time development shown here is depicted more completely by the computer movie printed in the upper right-hand corner of this issue. It can be seen by thumbing through the pages.

Ref. to "movie"

Fig. 8. Numerical triangle used to estimate value for $\langle n^3 \rangle$ in equation of motion for $\langle n^2 \rangle$ when the desired truncated set of moment equations includes only $\langle n \rangle$ and $\langle n^2 \rangle$. One sets the last difference equal to zero as given in Eq. (31). The estimate for $\langle n^{N+1} \rangle$ is given in terms of the first N moments by Eq. (32).

Fig. 9. Graphs of average photon number in time given by integration of truncated sets of N equations of motion from Eq. (25) and by the p_n("∞") integration according to Eq. (9).

Fig. 10. Graphs of mean square deviation in time obtained using the scheme for Fig. 9.

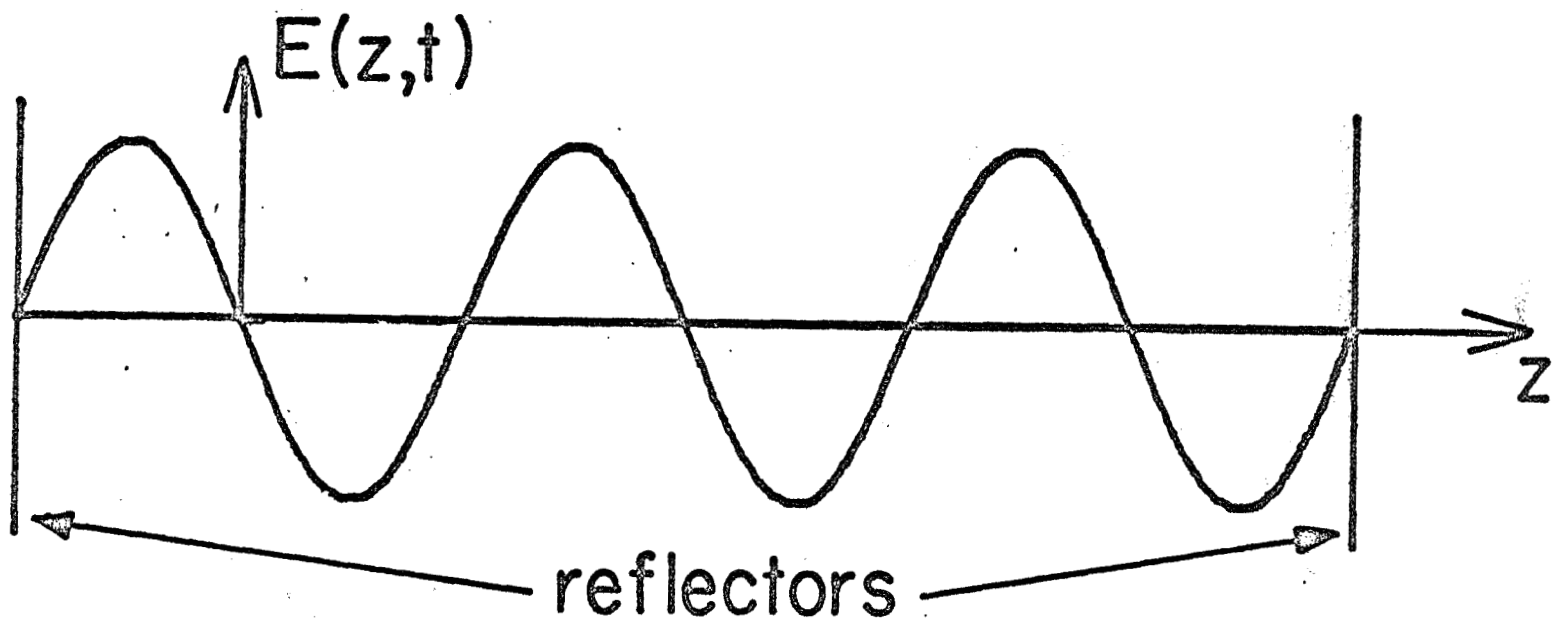
E(z,t)
z
reflectors

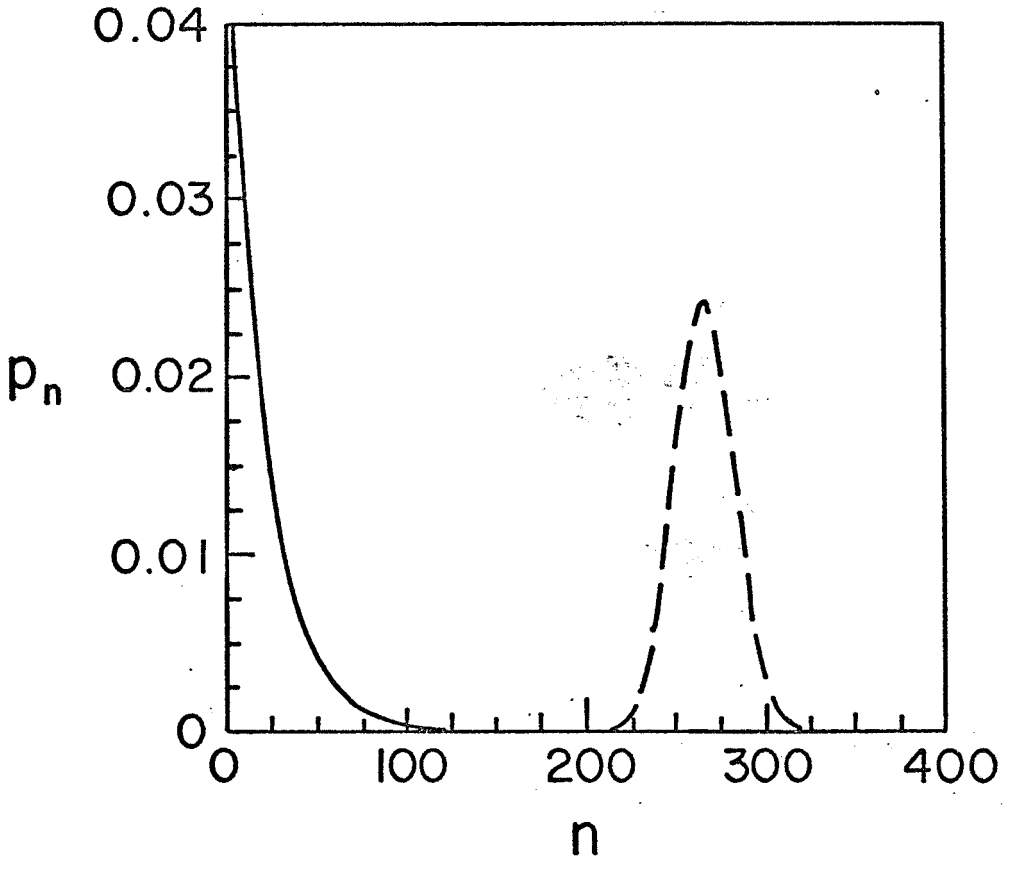
0.04
0.03
0.02
0.01
0
p_n
0
100
200
300
400
n

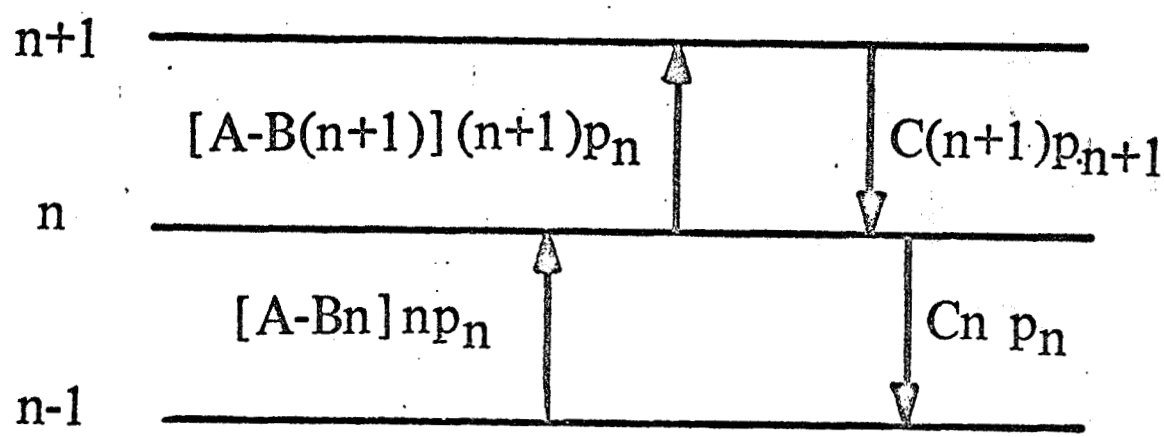
n+1
[A-B(n+1)] (n+1)p_n
C(n+1)p_{n+1}
n
[A-Bn] np_n
Cn p_n
n-1

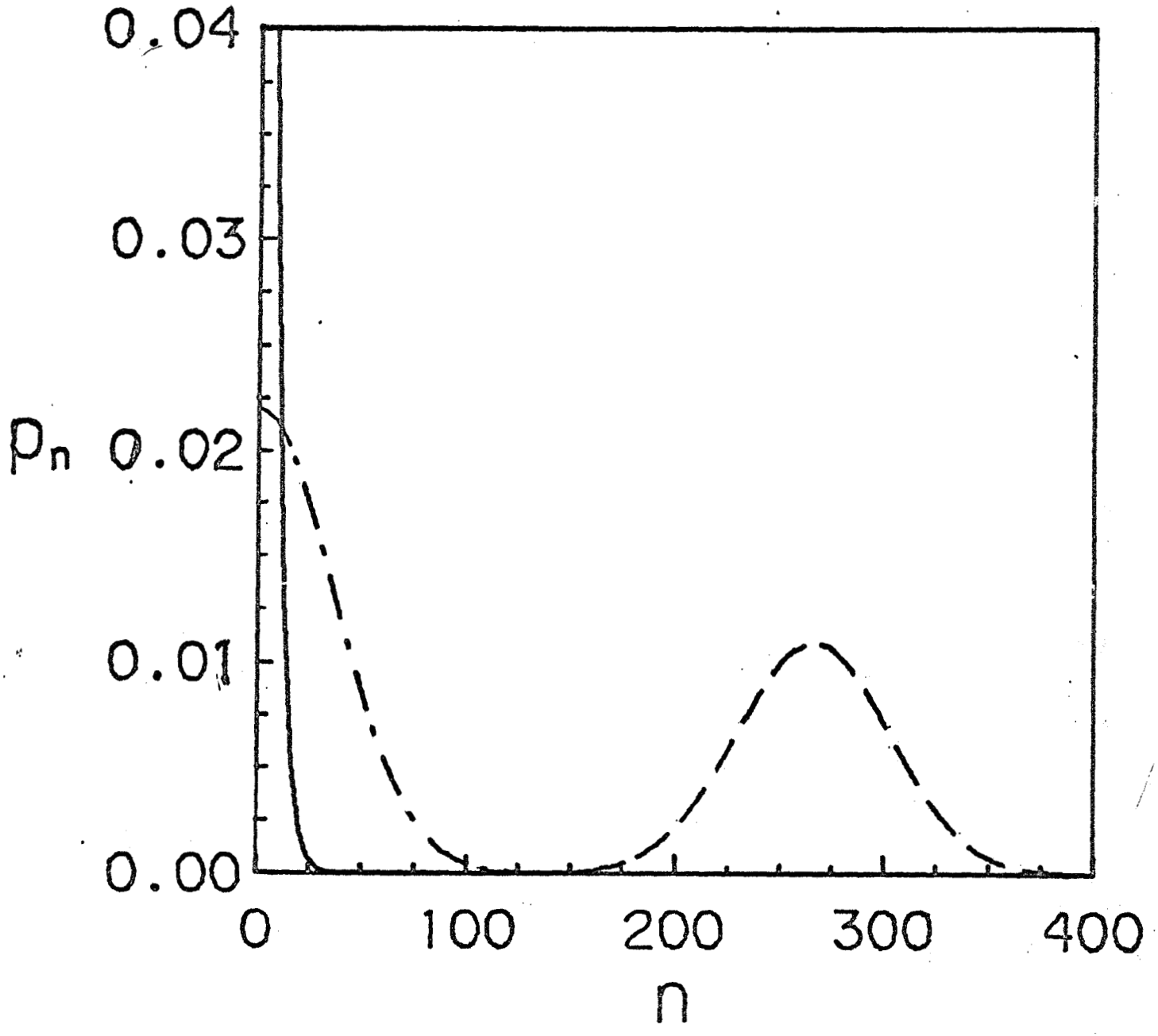
0.04
0.03
p_n 0.02
0.01
0.00
0
100
200
300
400
n

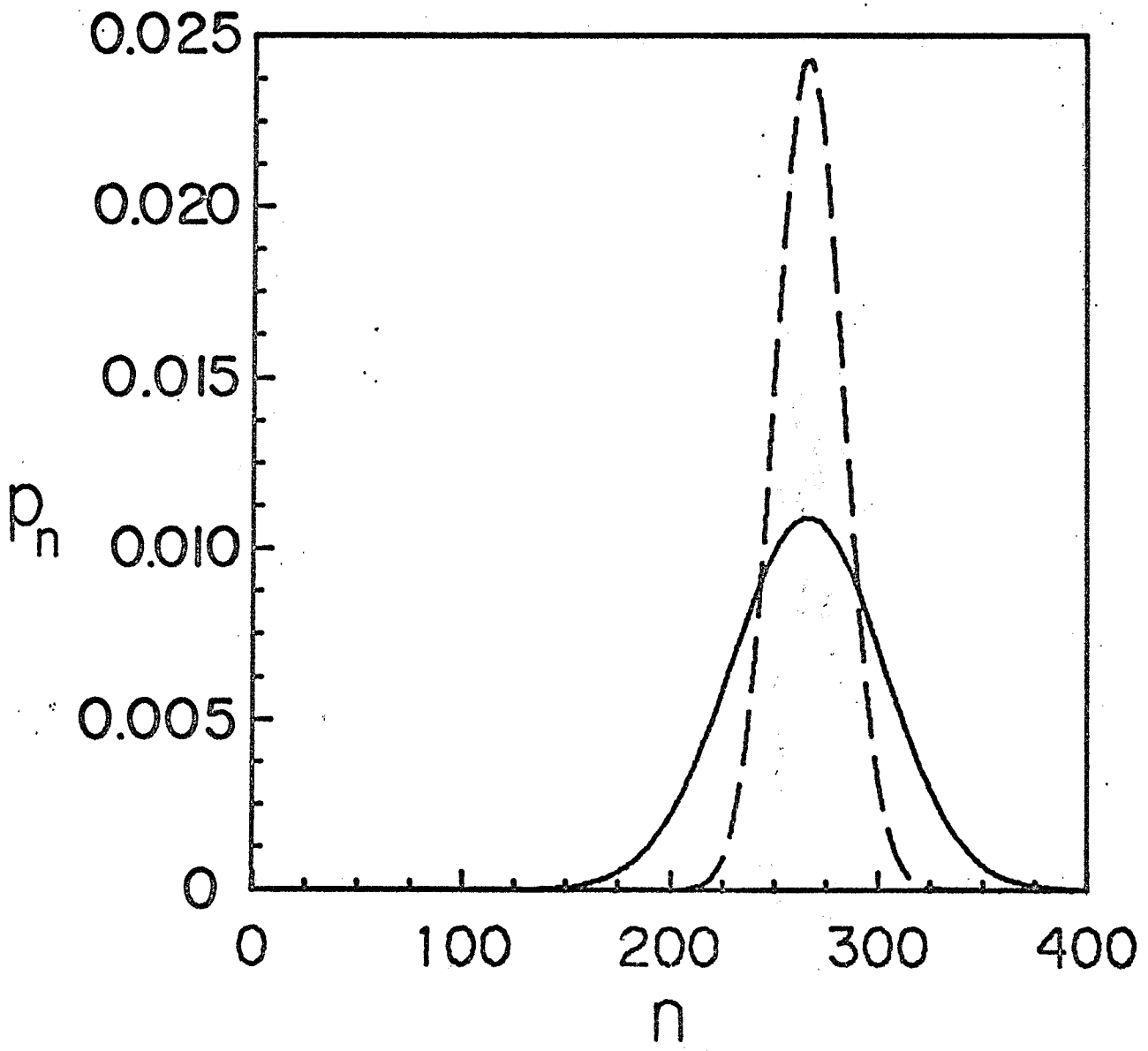
0.025
0.020
0.015
p_n
0.010
0.005
0
0
100
200
300
400
n

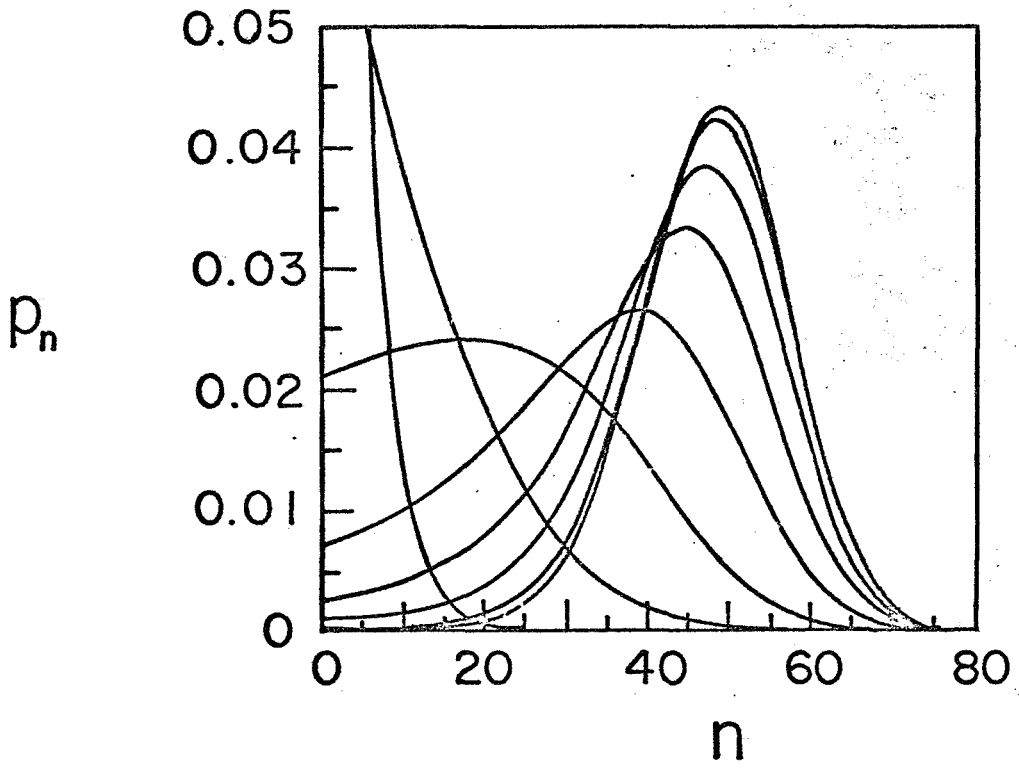
0.05
0.04
0.03
0.02
0.01
0
p_n
0
20
40
60
80
n

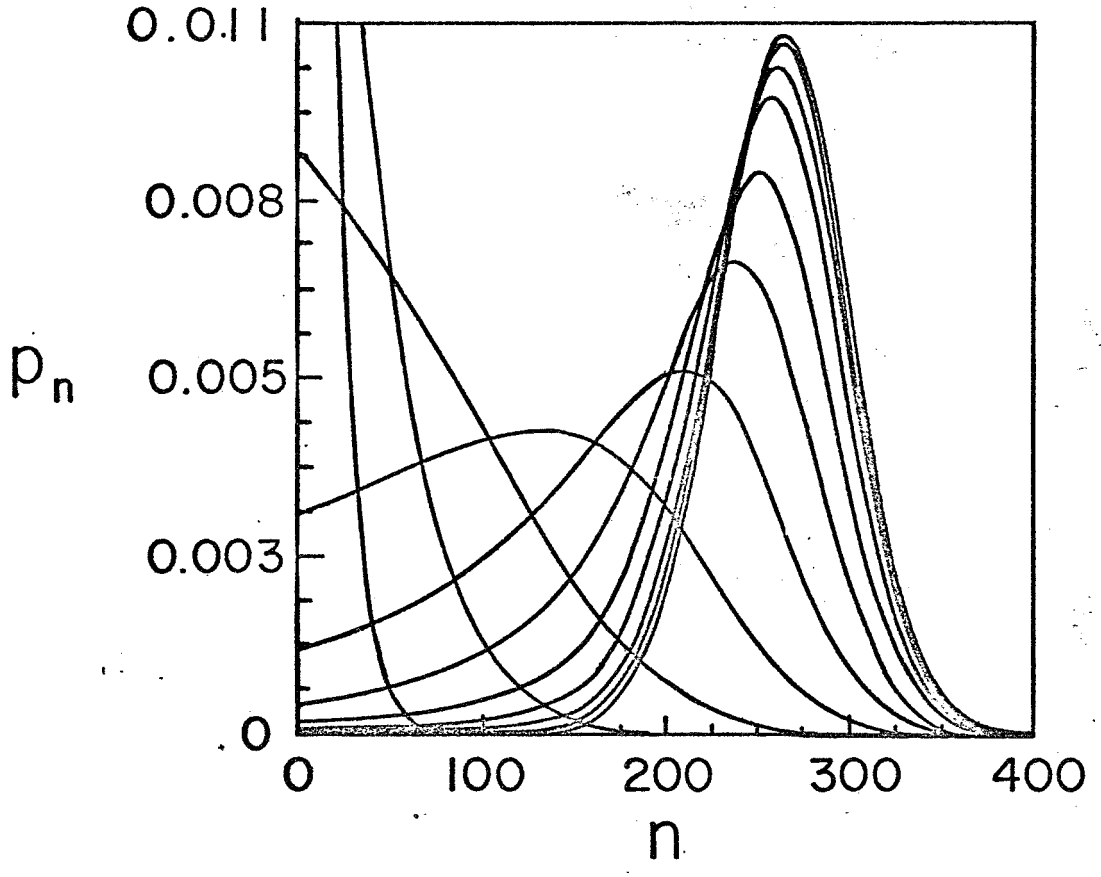
0.011
0.008
0.005
0.003
0
p_n
0
100
200
300
400
n

$\langle n \rangle$

$\langle n \rangle - \langle n^2 \rangle^{1/2}$

$\langle n^2 \rangle^{1/2}$ $\langle n \rangle + \langle n^3 \rangle^{1/3} - 2\langle n^2 \rangle^{1/2}$

$\langle n^2 \rangle^{1/2} - \langle n^3 \rangle^{1/3}$

$\langle n^3 \rangle^{1/3}$

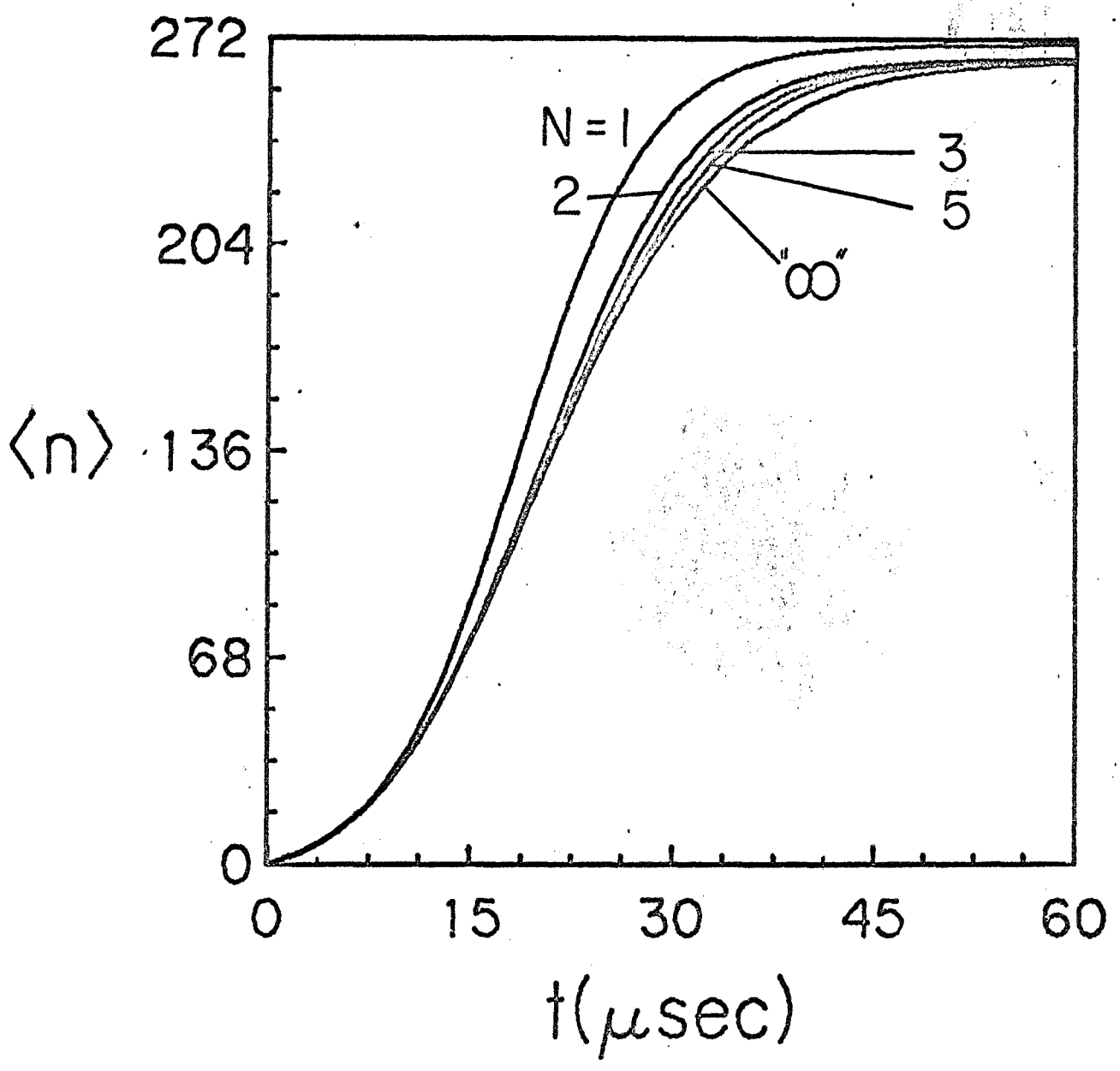
272
204
136
68
0
⟨n⟩
N = 1
2
3
5
"∞"
0
15
30
45
60
t(μsec)

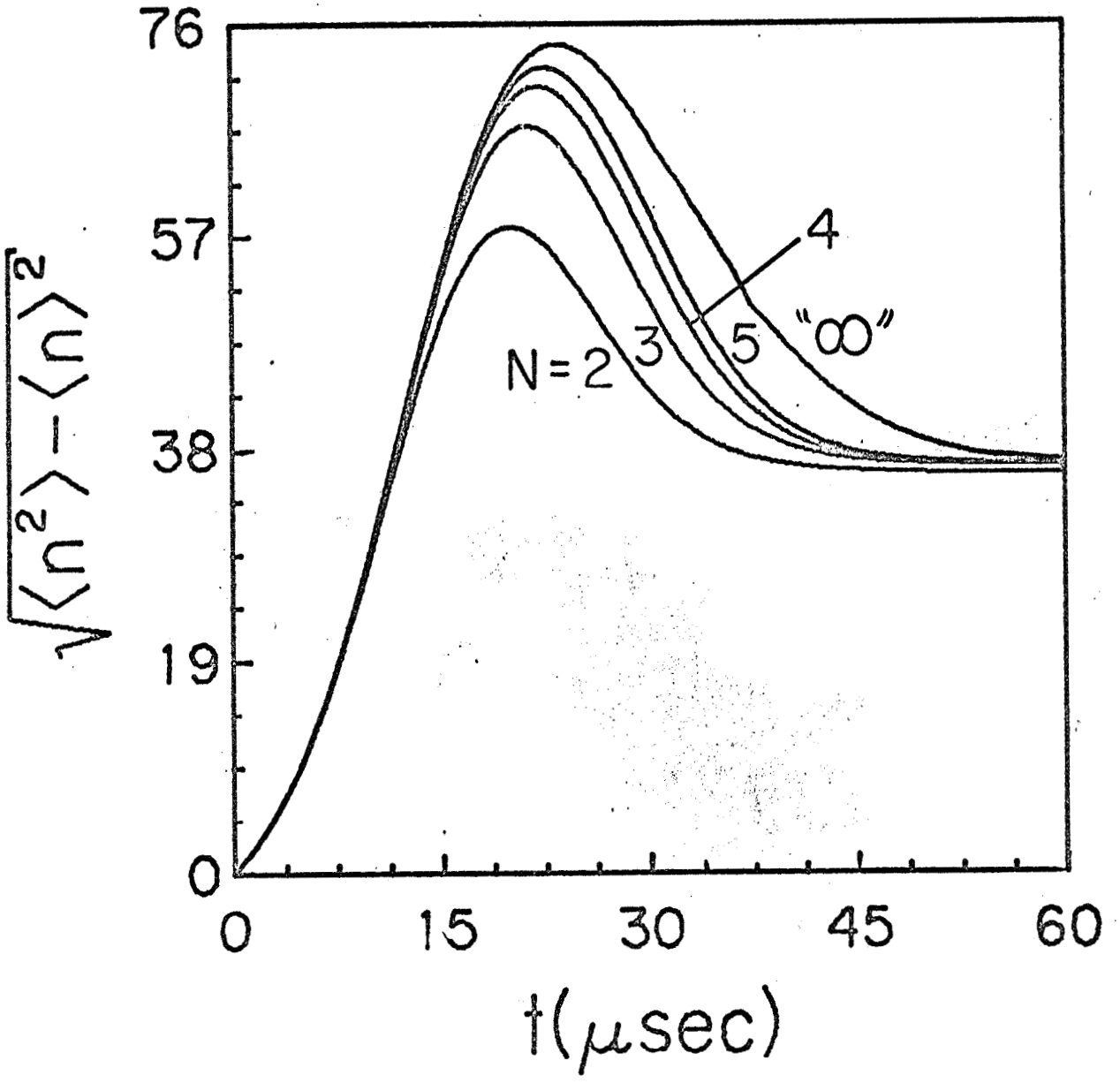
76
57
38
19
0
0
15
30
45
60
$\sqrt{\langle n^2\rangle - \langle n\rangle^2}$
t(μsec)
N=2
3
4
5
"∞"